PROCEEDINGS OF SCIENCE

Status and Prospect of SK-Gd Project

Y. Hino[a,*] **on behalf of the Super-Kamiokande collaboration**

[a] *Okayama University, Department of Physics,*
3-1-1 Tsushima-naka, Kita-ku, Okayama, 700-8530, Japan

E-mail: yotahino@okayama-u.ac.jp

In 2020, a new phase of Super-Kamiokande experiment, SK-Gd, was started by loading gadolinium into the pure water. This led to a high neutron detection efficiency, which allows us to distinguish different neutrino reactions, enhance signals and remove backgrounds more efficiently. In the summer of 2022, an update of SK-Gd was done by adding additional Gd, and thus totally 39 tonnes of gadolinium sulfate octahydrate has been introduced in the water. The Gd concentration was estimated as 0.0332±0.0002% based on the dissolved weight of gadolinium sulfate octahydrate powder. It is consistent with the result of the direct sampling from the detector as 334 ± 4 ppm. The spallation neutron measurement and AmBe calibration confirms the shorter capture time constant and higher capture event rate due to the second loading. Therefore, we achieved 1.5 times higher than that of the first loaded phase as expected.

38th International Cosmic Ray Conference (ICRC2023)
26 July - 3 August, 2023
Nagoya, Japan

*Speaker

PoS(ICRC2023)983

1. Introduction

The Super-Kamiokande (SK) [1] is the experiment held in Kamioka, Gifu, Japan. The detector contains 50 kilo-tonnes of ultra pure water and is placed in 1,000 m underground, i.e., 2,700 m water equivalent overburden. It is optically separated and forms the inner detector (ID) for observation and the outer detector (OD). The ID has 11,129 20-inch photomultiplier tubes (PMTs) to reconstruct the energy, generated position, direction and the kind of the charged particles. The OD with 1,885 8-inch PMTs identifies incoming cosmic ray muons. The rate of cosmic ray muon is reduced by a factor of 10^5 compared to that of the ground level. Therefore, it provides the appropriate environment to search for low energy events, e.g., solar neutrino and diffuse supernova background (DSNB). A new phase of the SK launched by loading gadolinium (Gd) which enhance the sensitivity to inverse beta decay (IBD) of electron anti-neutrino by detecting IBD neutron captured on Gd. We performed the first Gd loading [2] and achieved 0.01% Gd concentration as a initial step pf the SK-Gd project. Recently, the first DSNB search result using the full dataset (∼1.5 years) of the Gd 0.01% phase [3] has been reported and shows the sensitivity to the DSNB reached to the similar level to the decade observation in the pure water phase [4]. For further improvement, the second gadolinium loading to SK was conducted towards Gd concentration of 0.03%, resulting in more accurate supernova direction determination with an enhanced neutron detection efficiency.

2. The Second Gd Loading

During the second loading, 27.3 tons of $Gd_2(SO_4)_3 \cdot 8H_2O$ powder was dissolved into the detector. The powder contained an average of 4.4% additional water left over from processing. Therefore, the mass of $Gd_2(SO_4)_3 \cdot 8H_2O$ itself is 26.1 tons. This amount (plus Gd from the first loading) should yield a Gd concentration in the SK tank of 0.033%, equivalent to an anhydrous gadolinium sulfate ($Gd_2(SO_4)_3$) concentration of 0.079%. The $Gd_2(SO_4)_3 \cdot 8H_2O$ to be loaded into the SK is required to satisfy requirements from the solar neutrino observation and the DSNB search described in [5]. Thus, the mount of impurity in the powder must be assessed before they are dissolved into the SK water. Since the amount to be loaded is doubled from the first loading, we improved the loading equipment to speed up the process. In this section, the procedures of the screening and the loading are described.

2.1 Requirements and Screening

In order to assess the impurity in the $Gd_2(SO_4)_3 \cdot 8H_2O$, the chemical processing procedures were developed by an extensive R&D program which is also explained in [5]. Inductively Coupled Plasma Mass Spectrometry (ICP-MS) is used to assay U, Th, and Ce impurities prior to high-purity germanium (HPGe) gamma spectrometries. The procedure of the measurement is described in [5], and its sensitivity to the quantity of U and Th reaches at the parts-per-trillion (ppt) level. In addition to these assessment, we developed a new method to evaluate ^{222}Rn concentration using a chemical separation [6]. Since it can perform a relatively quick evaluation compared to the HPGe γ spectrometry, we applied it to the last two lots of $Gd_2(SO_4)_3 \cdot 8H_2O$ in order to keep the loading schedule. As a result of the screening, it was confirmed that all samples used in the second loading satisfies the criteria for U, Th, and Ce contamination.

2.2 Loading Equipment and Works

Figure 1 shows the improved dissolving system, which consists of the dissolving tank (4 m^3), the Gd injection port, and the shear mixer.

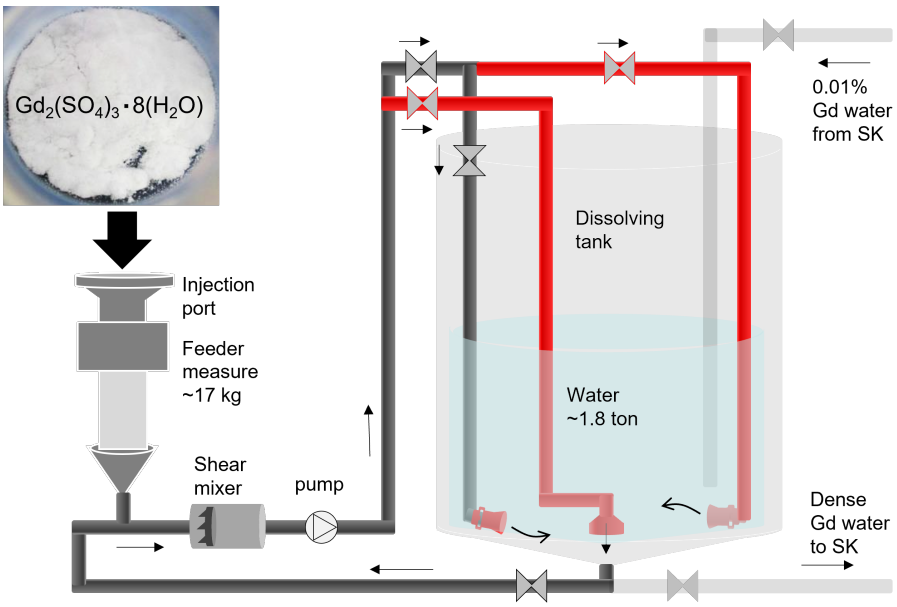

Figure 1: The schematic of the dissolving system. The parts added from the second loading are colored in red. In addition, the injection port was enlarged for the efficient Gd powder supplement.

Dissolving was done in the following procedure.
1. Supply $Gd_2(SO_4)_3 \cdot 8H_2O$ the feeder which monitors the weight of the powder from the injection port up to ~400 kg.
2. Fill the dissolving tank with ~1.8 m^3 of 0.01% water from the SK tank.
3. Circulate water between the shear mixer and the dissolving tank before dissolving.
4. The feeder supplies ~17 kg of $Gd_2(SO_4)_3 \cdot 8H_2O$ powder to the circulation line.
5. ~15 minutes circulation makes the powder dissolved into water.
6. Send the high concentration Gd water to the solution tank.

The high concentration dissolution will be diluted into 0.03% by mixing with the SK return water before being sent to the SK tank. The amount of powder and water are doubled from the previous loading in order to improve the loading speed twice. In order to achieve the requirement, we improved the dissolving system so as to achieve the requirement, as shown in Figure 1. The two L-shape pipe lines with a water ejector at their exit were placed to make a sufficiently powerful vortex preventing the powder from stagnating at the bottom of the dissolving tank without returning to the shear mixer. An increase in the number of the lines leads to a reduction of the discharge pressure at the circulation pump as well. We also added the pipe which goes directly to the exit of the tank efficiently returns the powder to the shear mixer. It was used at the first ~5 minutes of the dissolving process. This line was then partially closed, and the two L-shape lines are opened to make the vortex for the remaining 15 minutes. In addition to the dissolving system, the powder injection port was enlarged to make the powder injection work easier.

The second Gd loading took place from May 31 to July 4, 2022, i.e., 36 days operation in total. The accumulated weight of the supplied Gd sulfate power was 27304 kg corresponding to 10998 kg of Gd. It took approximately 25 minutes to dissolve 17 kg of Gd sulfate power in a batch, which shows the dissolving rate was doubled from 8.7 kg a batch in the first loading [2].

The expert workers refilled the reserve tank with Gd sulfate powder up to 400 kg every 8 hours. The lot number of each Gd powder were recorded in the refilling work. Thus, we can trace their radio-impurity based on the screening result. Figure 2 shows that a history of the total weight of Gd sulfate powder supplied to the feeder. It can be concluded that the loading work was smooth during the entire period because of the constant slope shown in the plot except for the one-day overhaul for pump maintenance on June 17, 2022.

The estimated weight of Gd in the SK water after the second loading was 16412 kg by taking a loss of Gd during the work and the existing Gd before the second loading into consideration. Therefore, the Gd concentration was 0.0332 ± 0.0002% as a result of the second loading. We assigned 0.5% uncertainty on both the weight of Gd and water.

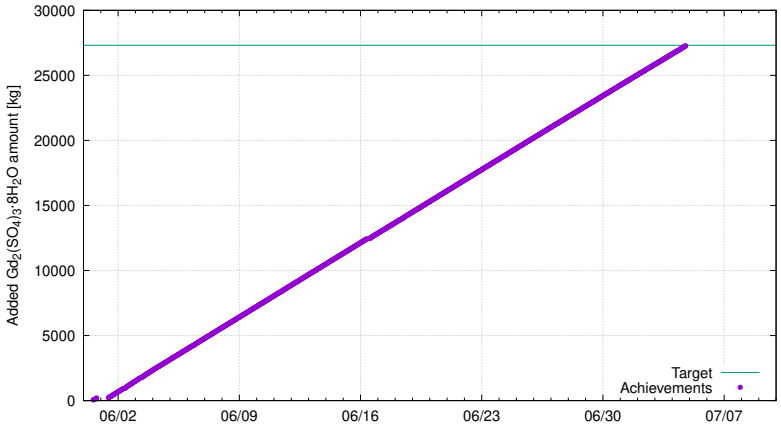

Figure 2: A plot showing that a history of the total weight of Gd sulfate powder added into the SK water. The horizontal line colored in light blue indicates the goal of T1.5 (~ 27.3 tonnes). We achieved it on July 4th, 2022.

3. Gd Concentration Monitoring

3.1 Spallation neutron induced by cosmic muon

We performed the Gd concentration monitoring while and after the loading by detecting neutrons produced by spallation reaction of ^{16}O induced by cosmic muons, called spallation neutrons. The effect of Gd concentration can appear as the shorting of the neutron capture time constant as well as the increase of the number of neutrons captured by Gd. Selection of spallation neutrons is done with a method described in [7]. An SHE trigger was generated whenever more than 60 ID PMT hits within a 200 ns time window. These SHE triggers resulted in all PMT hits within the 35 μs around the SHE trigger being recorded, while those in a subsequent 500 μs window were also recorded by a sequentially issued AFT trigger. Cosmic muons passing through the SK detector

were triggered by requiring both SHE trigger and the OD activity. Neutron event candidates are searched from subsequent PMT hits within the 35 μs SHE trigger window and the following 500 μs AFT trigger window.

Figure 3 shows spacial distributions of spallation neutron candidates for each week after the start of the second Gd loading. It clearly shows that the region with a higher density of neutron candidate gradually expands from the bottom, at a rate consistent with the water recirculation rate.

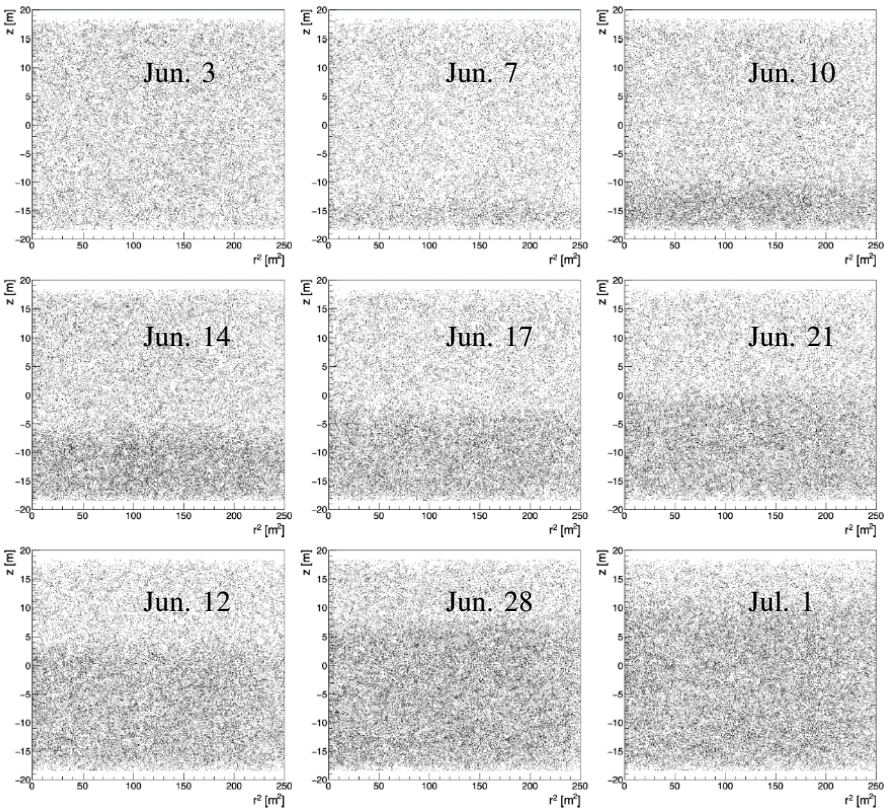

Figure 3: The plots showing the spatial distribution of the neutron capture events from cosmic ray spallation. The nine panels exhibit that the dense event region corresponding to the additionally loaded water gradually climbed as a function of time.

The event rate of the spallation induced neutron capture is estimated as 80.0 ± 9.0 /hour, which is 1.5 larger than the rate in Gd 0.01% configuration (56.1 ± 7.5 /hour). It directly indicates that an increase in the Gd concentration as a result of the second loading. The neutron tagging efficiency is evaluated using the Americium-Beryllium (AmBe) neutron source described in the following subsection.

3.2 AmBe neutron source

The advantage of using an AmBe source lies in the ability to identify its neutron emission due to the coincident emission of a 4.4 MeV gamma-ray. Placing the AmBe source within a $5\times5\times5$ cm BGO crystal cube allowed the initial gamma-ray to be detected by SK from the large number of scintillation photons generated by its passage through the BGO.

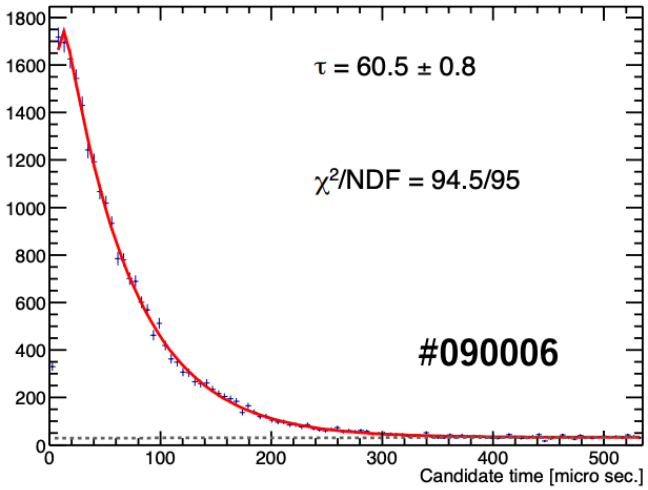

Figure 4: An example of the time distribution of neutron capture events in the AmBe data. The source was deployed at $z = -12$ m. The red line shows the curve fitting with the function considering the neutron thermalization and capture time constants. The capture time was estimated as 60.5 ± 0.8 μs.

The time distribution of neutron capture event candidates are shown in Figure 4. The event candidates of neutron capture on Gd were then extracted from this recorded data by looking for greater than 25 active PMTs in a 200 ns time window and applying event vertex reconstruction. In addition, we required the initial SHE trigger events containing 900 to 1200 p.e. charge in order to identify scintillation light from 4.4 MeV gamma-ray as a prompt signal. The following event selection was applied for the neutron event candidates using the event reconstruction parameters: the reconstruction timing goodness had to be greater than 0.4, the hit pattern goodness smaller than 0.4, and the event vertex located within 3 m from the AmBe source position.

A curve fitting taking neutron thermalization and capture time as well as accidental coincidence background component was performed in order to extract the capture time constant. The fit result gives the capture lifetime of 60.5 ± 0.8 μs, which corresponds to the neutron tagging efficiency of 51.8 ± 0.3%.

Figure 5 shows the result of weekly AmBe measurement. We deployed the AmBe source at the several positions along the z axis at each measurement for crosschecking the concentration monitoring using cosmic spallation neutron. One can find that the high concentration region gradually climbed along the z axis as a function of time, which is consistent with the observation of the spallation neutron. The regular AmBe measurement after the loading shows the capture time constant is stable over 5 months. Thus, we continues the stable operation in the SK-VII phase.

3.3 Sampling

During the second loading, we collected samples from both the ID and the OD twice a week. Figure 6 shows the result of conductivity measurements for each sample collected at the multiple positions along the z axis. It displays the high conductivity region sequentially climbs as a function of time, which is consistent with the observation in both the spallation neutron and AmBe measurements. The collected samples are then analysed with an Atomic Absorption Spectrometer

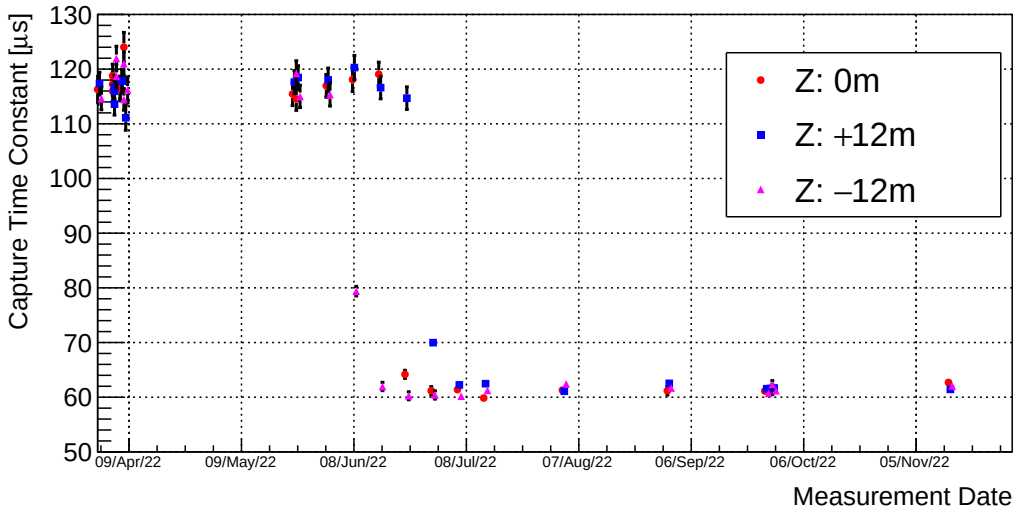

Figure 5: Weekly measured capture time constant using the AmBe source at several z positions. One can find an increase in the Gd concentration due to the shorter capture time constant as the result of the second loading.

(AAS) to determine the Gd concentration. In order to calibrate the measured concentration, 10 and 20 ppm standard sample made with the $Gd_2(SO_4)_3 \cdot 8H_2O$ used in the second loading were used. At the end of the loading, $Gd_2(SO_4)_3 \cdot 8H_2O$ is homogeneous in the SK detector with an average value of 793 ± 9 ppm. The Gd only concentration can be computed as 334 ± 4 ppm by the stoichiometric calculation.

4. Summary

For a further increase in the neutron capture efficiency from 50% to 75%, 26.1 tons of $Gd_2(SO_4)_3 \cdot 8H_2O$ was additionally loaded to SK from May 31 to July 4, 2022. As the amount of loaded $Gd_2(SO_4)_3 \cdot 8H_2O$ was doubled compared to the first loading, the capacity of the powder dissolving system was doubled. We also developed new batches of gadolinium sulfate with the further reduction of radioactive impurities. A more efficient screening method was also developed and implemented for the evaluation. The Gd concentration was measured to be 334 ± 4 ppm by the AAS, which is in good agreement with 0.0332 ± 0.0002% by the estimation based on the weight measurement. Furthermore, the Gd concentration was monitored sequentially using the capture time constants of each spallation neutron produced by the cosmic-ray muon during the loading of Gd, and the neutron capture efficiency was shown to become 1.5 times higher than that of the first loaded phase as expected. We are stably operating the SK-VII phase in terms of the Gd concentration ensured by the regular AmBe calibration.

References

[1] S. Fukuda *et al.*, The Super-Kamiokande detector, Nucl. Instrum. Methods A 501 (2003) 418-462.

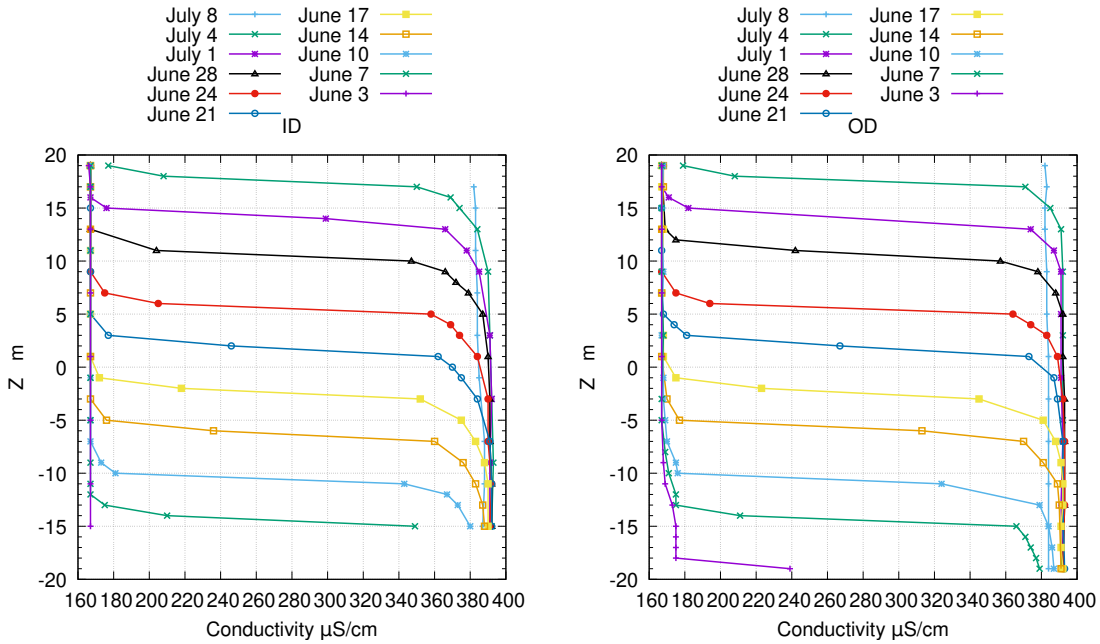

Figure 6: The result of conductivity measurements for samples from the ID (left) and the OD (right). We collected the samples at the multiple positions along the z axis. It displays the high conductivity region sequentially climbs as a function of time, which is consistent with the observation in both the spallation neutron and AmBe measurements.

[2] K. Abe *et al.*, First gadolinium loading to Super-Kamiokande, Nucl. Instrum. Methods A 1027 (2022) 166248

[3] M. Harada *et al.*, Search for astrophysical electron antineutrinos in Super-Kamiokande with 0.01wt% gadolinium-loaded water, 2023 ApJL 951 L27.

[4] K. Abe *et al.* (Super-Kamiokande Collaboration), Diffuse Supernova neutrino background search at Super-Kamiokande, Phys. Rev. D 104, 122002.

[5] K. Hosokawa *et al.*, Development of ultra-pure gadolinium sulfate for the Super-Kamiokande gadolinium project, Progress of Theoretical and Experimental Physics, Volume 2023, Issue 1, January 2023, 013H01

[6] Y. Sakakieda *et al.*, Rapid Analysis of ^{226}Ra in Ultrapure Gadolinium Sulfate Octahydrate, arXiv.2306.06926

[7] M. Shinoki *et al.* (Super-Kamiokande Collaboration), Measurement of the cosmogenic neutron yield in Super-Kamiokande with gadolinium loaded water, Phys. Rev. D 107, 092009.

Full Authors List: Super-Kamiokande Collaboration

K. Abe[1,46], C. Bronner[1], Y. Hayato[1,46], K. Hiraide[1,46], K. Hosokawa[1], K. Ieki[1,46], M. Ikeda[1,46], J. Kameda[1,46], Y. Kanemura[1], R. Kaneshima[1], Y. Kashiwagi[1], Y. Kataoka[1,46], S. Miki[1], S. Mine[1,46], M. Miura[1,46], S. Moriyama[1,46], Y. Nakano[1], M. Nakahata[1,46], S. Nakayama[1,46], Y. Noguchi[1], K. Sato[1], H. Sekiya[1,46], H. Shiba[1], K. Shimizu[1], M. Shiozawa[1,46], Y. Sonoda[1], Y. Suzuki[1], A. Takeda[1,46], Y. Takemoto[1,46], H. Tanaka[1,46], T. Yano[1], S. Han[2], T. Kajita[2,22,46], K. Okumura[2,46], T. Tashiro[2], T. Tomiya[2], X. Wang[2], S. Yoshida[2], P. Fernandez[3], L. Labarga[3], N. Ospina[3], B. Zaldivar[3], B. W. Pointon[4,49], E. Kearns[5,46], J. L. Raaf[5], L. Wan[5], T. Wester[5], J. Bian[6], N. J. Griskevich[6], S. Locke[6], M. B. Smy[6,46], H. W. Sobel[6,46], V. Takhistov[6,24], A. Yankelevich[6], J. Hill[7], S. H. Lee[8], D. H. Moon[8], R. G. Park[8], B. Bodur[9], K. Scholberg[9,46], C. W. Walter[9,46], A. Beauchê,ne[10], O. Drapier[10], A. Giampaolo[10], Th. A. Mueller[10], A. D. Santos[10], P. Paganini[10], B. Quilain[10], T. Nakamura[11], J. S. Jang[12], L. N. Machado[13], J. G. Learned[14], K. Choi[15], N. Iovine[15], S. Cao[16], L. H. V. Anthony[17], D. Martin[17], N. W. Prouse[17], M. Scott[17], A. A. Sztuc[17], Y. Uchida[17], V. Berardi[18], M. G. Catanesi[18], E. Radicioni[18], N. F. Calabria[19], A. Langella[19], G. De Rosa[19], G. Collazuol[20], F. Iacob[20], M. Mattiazzi[20], L. Ludovici[21], M. Gonin[22], G. Pronost[22], C. Fujisawa[23], Y. Maekawa[23], Y. Nishimura[23], R. Okazaki[23], R. Akutsu[24], M. Friend[24], T. Hasegawa[24], T. Ishida[24], T. Kobayashi[24], M. Jakkapu[24], T. Matsubara[24], T. Nakadaira[24], K. Nakamura[24,46], Y. Oyama[24], K. Sakashita[24], T. Sekiguchi[24], T. Tsukamoto[24], N. Bhuiyan[25], G. T. Burton[25], F. Di Lodovico[25], J. Gao[25], A. Goldsack[25], T. Katori[25], J. Migenda[25], Z. Xie[25], S. Zsoldos[25,46], A. T. Suzuki[26], Y. Takagi[26], Y. Takeuchi[26,46], J. Feng[27], L. Feng[27], J. R. Hu[27], Z. Hu[27], T. Kikawa[27], M. Mori[27], T. Nakaya[27,46], R. A. Wendell[27,46], K. Yasutome[27], S. J. Jenkins[28], N. McCauley[28], P. Mehta[28], A. Tarant[28], Y. Fukuda[29], Y. Itow[30,31], H. Menjo[30], K. Ninomiya[30], J. Lagoda[32], S. M. Lakshmi[32], M. Mandal[32], P. Mijakowski[32], Y. S. Prabhu[32], J. Zalipska[32], M. Jia[33], J. Jiang[33], C. K. Jung[33], M. J. Wilking[33], C. Yanagisawa[33*], M. Harada[34], Y. Hino[34], H. Ishino[34], Y. Koshio[34,46], F. Nakanishi[34], S. Sakai[34], T. Tada[34], T. Tano[34], T. Ishizuka[35], G. Barr[36], D. Barrow[36], L. Cook[36,46], S. Samani[36], D. Wark[36,41], A. Holin[37], F. Nova[37], B. S. Yang[38], J. Y. Yang[38], J. Yoo[38], J. E. P. Fannon[39], L. Kneale[39], M. Malek[39], J. M. McElwee[39], M. D. Thiesse[39], L. F. Thompson[39], S. T. Wilson[39], H. Okazawa[40], S. B. Kim[42], E. Kwon[42], J. W. Seo[42], I. Yu[42], A. K. Ichikawa[43], K. D. Nakamura[43], S. Tairafune[43], K. Nishijima[44], A. Eguchi[45], K. Nakagiri[45], Y. Nakajima[45,46], S. Shima[45], N. Taniuchi[45], E. Watanabe[45], M. Yokoyama[45,46], P. de Perio[46], S. Fujita[46], K. Martens[46], K. M. Tsui[46], M. R. Vagins[46,6], J. Xia[46], S. Izumiyama[47], M. Kuze[47], R. Matsumoto[47], M. Ishitsuka[48], H. Ito[48], Y. Ommura[48], N. Shigeta[48], M. Shinoki[48], K. Yamauchi[48], T. Yoshida[48], R. Gaur[49], V. Gousy-Leblanc[49†], M. Hartz[49], A. Konaka[49], X. Li[49], S. Chen[50], B. D. Xu[50], B. Zhang[50], M. Posiadala-Zezula[51], S. B. Boyd[52], R. Edwards[52], D. Hadley[52], M. Nicholson[52], M. O'Flaherty[52], B. Richards[52], A. Ali[53,49], B. Jamieson[53], S. Amanai[54], Ll. Marti[54], A. Minamino[54], S. Suzuki[54]

[1] Kamioka Observatory, Institute for Cosmic Ray Research, University of Tokyo, Kamioka, Gifu 506-1205, Japan
[2] Research Center for Cosmic Neutrinos, Institute for Cosmic Ray Research, University of Tokyo, Kashiwa, Chiba 277-8582, Japan
[3] Department of Theoretical Physics, University Autonoma Madrid, 28049 Madrid, Spain
[4] Department of Physics, British Columbia Institute of Technology, Burnaby, BC, V5G 3H2, Canada
[5] Department of Physics, Boston University, Boston, MA 02215, USA
[6] Department of Physics and Astronomy, University of California, Irvine, Irvine, CA 92697-4575, USA
[7] Department of Physics, California State University, Dominguez Hills, Carson, CA 90747, USA
[8] Institute for Universe and Elementary Particles, Chonnam National University, Gwangju 61186, Korea
[9] Department of Physics, Duke University, Durham NC 27708, USA
[10] Ecole Polytechnique, IN2P3-CNRS, Laboratoire Leprince-Ringuet, F-91120 Palaiseau, France
[11] Department of Physics, Gifu University, Gifu, Gifu 501-1193, Japan
[12] GIST College, Gwangju Institute of Science and Technology, Gwangju 500-712, Korea
[13] School of Physics and Astronomy, University of Glasgow, Glasgow, Scotland, G12 8QQ, United Kingdom
[14] Department of Physics and Astronomy, University of Hawaii, Honolulu, HI 96822, USA
[15] Center for Underground Physics, Institute for Basic Science (IBS), Daejeon, 34126, Korea
[16] Institute For Interdisciplinary Research in Science and Education, ICISE, Quy Nhon, 55121, Vietnam
[17] Department of Physics, Imperial College London , London, SW7 2AZ, United Kingdom
[18] Dipartimento Interuniversitario di Fisica, INFN Sezione di Bari and Università e Politecnico di Bari, I-70125, Bari, Italy
[19] Dipartimento di Fisica, INFN Sezione di Napoli and Università di Napoli, I-80126, Napoli, Italy
[20] Dipartimento di Fisica, INFN Sezione di Padova and Università di Padova, I-35131, Padova, Italy
[21] INFN Sezione di Roma and Università di Roma "La Sapienza", I-00185, Roma, Italy
[22] ILANCE, CNRS - University of Tokyo International Research Laboratory, Kashiwa, Chiba 277-8582, Japan
[23] Department of Physics, Keio University, Yokohama, Kanagawa, 223-8522, Japan
[24] High Energy Accelerator Research Organization (KEK), Tsukuba, Ibaraki 305-0801, Japan
[25] Department of Physics, King's College London, London, WC2R 2LS, UK
[26] Department of Physics, Kobe University, Kobe, Hyogo 657-8501, Japan
[27] Department of Physics, Kyoto University, Kyoto, Kyoto 606-8502, Japan
[28] Department of Physics, University of Liverpool, Liverpool, L69 7ZE, United Kingdom

*also at BMCC/CUNY, Science Department, New York, New York, 1007, USA
†also at University of Victoria, Department of Physics and Astronomy, PO Box 1700 STN CSC, Victoria, BC V8W 2Y2, Canada

[29] Department of Physics, Miyagi University of Education, Sendai, Miyagi 980-0845, Japan
[30] Institute for Space-Earth Environmental Research, Nagoya University, Nagoya, Aichi 464-8602, Japan
[31] Kobayashi-Maskawa Institute for the Origin of Particles and the Universe, Nagoya University, Nagoya, Aichi 464-8602, Japan
[32] National Centre For Nuclear Research, 02-093 Warsaw, Poland
[33] Department of Physics and Astronomy, State University of New York at Stony Brook, NY 11794-3800, USA
[34] Department of Physics, Okayama University, Okayama, Okayama 700-8530, Japan
[35] Media Communication Center, Osaka Electro-Communication University, Neyagawa, Osaka, 572-8530, Japan
[36] Department of Physics, Oxford University, Oxford, OX1 3PU, United Kingdom
[37] Rutherford Appleton Laboratory, Harwell, Oxford, OX11 0QX, UK
[38] Department of Physics, Seoul National University, Seoul 151-742, Korea
[39] Department of Physics and Astronomy, University of Sheffield, S3 7RH, Sheffield, United Kingdom
[40] Department of Informatics in Social Welfare, Shizuoka University of Welfare, Yaizu, Shizuoka, 425-8611, Japan
[41] STFC, Rutherford Appleton Laboratory, Harwell Oxford, and Daresbury Laboratory, Warrington, OX11 0QX, United Kingdom
[42] Department of Physics, Sungkyunkwan University, Suwon 440-746, Korea
[43] Department of Physics, Faculty of Science, Tohoku University, Sendai, Miyagi, 980-8578, Japan
[44] Department of Physics, Tokai University, Hiratsuka, Kanagawa 259-1292, Japan
[45] Department of Physics, University of Tokyo, Bunkyo, Tokyo 113-0033, Japan
[46] Kavli Institute for the Physics and Mathematics of the Universe (WPI), The University of Tokyo Institutes for Advanced Study, University of Tokyo, Kashiwa, Chiba 277-8583, Japan
[47] Department of Physics,Tokyo Institute of Technology, Meguro, Tokyo 152-8551, Japan
[48] Department of Physics, Faculty of Science and Technology, Tokyo University of Science, Noda, Chiba 278-8510, Japan
[49] TRIUMF, 4004 Wesbrook Mall, Vancouver, BC, V6T2A3, Canada
[50] Department of Engineering Physics, Tsinghua University, Beijing, 100084, China
[51] Faculty of Physics, University of Warsaw, Warsaw, 02-093, Poland
[52] Department of Physics, University of Warwick, Coventry, CV4 7AL, UK
[53] Department of Physics, University of Winnipeg, MB R3J 3L8, Canada
[54] Department of Physics, Yokohama National University, Yokohama, Kanagawa, 240-8501, Japan